Journal of Scientific Research & Reports
12(4): 1-9, 2016; Article no.JSRR.29802
ISSN: 2320-0227

SCIENCEDOMAIN *international*
www.sciencedomain.org

Design Approach for 2D Recursive Filters Used in Frequency Plane Partitioning

Radu Matei[1*]

[1]*Faculty of Electronics, Telecommunications and Information Technology, "Gheorghe Asachi" Technical University, Bd. Carol I nr.11, Iasi, Romania.*

Author's contribution

The sole author designed, analyzed and interpreted and prepared the manuscript.

Article Information

DOI: 10.9734/JSRR/2016/29802
Editor(s):
(1) Grigorios L. Kyriakopoulos, School of Electrical and Computer Engineering, National Technical University of Athens (NTUA), Greece.
Reviewers:
(1) Moumi Pandit, Sikkim Manipal University, India.
(2) Shilpi Birla, Manipal University, Jaipur, India.
Complete Peer review History: http://www.sciencedomain.org/review-history/16784

Original Research Article

Received 29th September 2016
Accepted 29th October 2016
Published 4th November 2016

ABSTRACT

This work proposes an analytical design procedure for some types of 2D recursive filters useful in frequency plane partitioning, namely diamond, parallelogram, fan or wedge-shaped filters with a specified bandwidth and orientation. Such filters can be used as components of particular filter banks, applied in directional image decomposition. The design starts from two zero-phase low-pass 1D prototypes, to which specific frequency mappings are applied, also exploiting the symmetry properties in the frequency plane. This method combines analytical approach with numerical approximations, yielding the desired 2D frequency response. A more selective filter results by combining two or several elementary filters. Several design examples for these filters are provided.

Keywords: 2D IIR filters; directional filters; frequency mapping; approximation.

1. INTRODUCTION

Various design methods for 2D filters, both FIR and IIR, have been proposed by many researchers and are now well founded [1,2]. A frequently-used design technique is based on a specified 1D prototype filter, whose transfer function is transformed using various frequency mappings to obtain a 2D filter with desired shape. Some early papers on 2D filter design

**Corresponding author: E-mail: rmatei@etti.tuiasi.ro;*

using spectral transformations are [3,4]. Some authors have used optimization methods to design 2D filters with arbitrary frequency response, like in [5]. The stability issue for 2D filters and some stabilization methods are treated in papers like [6,7]. Diamond filters are currently used as anti-aliasing filters for conversion of sampled signals from rectangular to quincunx sampling grid. Different design methods for diamond filters were studied in various papers like [8-10].

In [11] a filter bank for the directional decomposition of images was proposed. The Bamberger directional filter bank [12] is an oriented image decomposition with very good selectivity and low computational complexity. It splits the frequency plane into wedge-shaped channels with *N* = 2, 4, 6 and 8 sub-bands, each capturing spatial details along a specific orientation. Fig. 2 (a) shows the 8-band frequency partition. Wedge and fan filters, combined with pattern recognition techniques, are applied in feature extraction, for instance in texture classification. Recently, some authors have proposed the more general class of nonuniform directional filter banks, with arbitrary frequency partitioning or number of sub-bands [13,14].

Various efficient design procedures for FIR and IIR fan filters were approached in early works like [15,16]. Some analytical methods were proposed by the author for the design of adjustable square-shaped filters [17] and wedge filters [18], using specific frequency mappings and various approximations.

This paper proposes a novel analytical method for the design of various 2D filters for frequency plane partition, namely with diamond, parallelogram, fan or wedge-shaped frequency response, starting from two zero-phase low-pass prototype filters and applying specific frequency mappings. The proposed design approach is mainly analytical, but also uses some efficient approximations. Section 2 presents the prototype filters used, while in Section 3 the design of diamond and fan filters is detailed. More general filters, like parallelogram and wedge filters are derived in Section 4.

2. PROTOTYPES FOR DIAMOND AND FAN-SHAPED 2D FILTERS

Generally, analytical design methods are based on 1D filters with imposed parameters, which are prototypes for the desired 2D filters. In this section, two zero-phase low-pass (LP) prototype filters will be discussed and will be used in the proposed design approach. First, let us consider a continuous function with odd parity approximating a step function, namely hyperbolic tangent $H_{HT}(\omega) = \tanh(10 \cdot \omega)$. In order to find a trigonometric approximation of $H_{HT}(\omega)$ the following variable change is introduced:

$$\omega = \arcsin\left(x/\pi\right) \;\leftrightarrow\; x = \pi \sin(\omega) \tag{1}$$

Using the Chebyshev-Padé method, we can easily derive the following trigonometric approximation for $\omega \in (-\pi, \pi)$:

$$H_1(\omega) = 1.265 \cdot \frac{(\sin\omega)(1 - 0.687922\cos 2\omega)}{(1 - 1.062289\cos 2\omega + 0.105738\cos 4\omega)} \tag{2}$$

which is displayed in Fig. 1 (a). This smooth, maximally-flat function will be further used as a prototype for particular diamond and fan filters.

For the second prototype, let us consider a Butterworth low-pass filter $H_B(s)$ of order *N,* with transfer function magnitude of the form $|H_B(j\omega)| = 1/\sqrt{1 + (\omega/\omega_0)^{2N}}$, where ω_0 is the cut-off frequency of the filter. Its magnitude in normalized frequency $(\omega_0 = 1)$ is the function $|H_{Bn}(j\omega)|$ [2]:

$$|H_{Bn}(j\omega)| = 1/\sqrt{1 + \omega^{2N}} \tag{3}$$

In order to obtain a zero-phase prototype of the same shape as $|H_{Bn}(j\omega)|$, a rational approximation of the magnitude $|H_{Bn}(j\omega)|$ for $\omega \in [-\pi, \pi]$ is needed. A convenient method is the Chebyshev-Padé expansion; it yields an efficient and uniform approximation over a specified interval and can be found using a symbolic computation software like MAPLE. Since a filter with a steeper characteristic would be desirable, let us take an order $N = 12$ and we get for $\omega \in [-\pi, \pi]$ the 8-th order rational approximation of the magnitude in factored form, also used in [17]:

$$\frac{1}{\sqrt{1+\omega^{24}}} \cong H_P(\omega) = \xi \cdot \frac{(\omega^4 - 5.8589322 \cdot \omega^2 + 22.393616)}{(\omega^4 + 0.253253 \cdot \omega^2 + 0.2830378)} \cdot \frac{(\omega^4 - 13.689786 \cdot \omega^2 + 49.701196)}{(\omega^4 - 1.843889 \cdot \omega^2 + 0.999034)} \quad (4)$$
$$= \xi \cdot H_{P1}(\omega) \cdot H_{P2}(\omega)$$

where $\xi = 0.0002516$. The frequency response $H_P(\omega)$ of this prototype is plotted in Fig. 1 (b) and shows a small amplitude ripple in the pass-band. The cut-off frequency is $\omega_0 = 1$ and $p = 1$. A low-pass filter with a better flatness would obviously result of higher order. The advantage of this factored rational approximation is that it is easily scalable on frequency axis. Each of the rational expressions $H_{Pi}(\omega)$ (for $i = 1, 2, \ldots$) occurring as factors in $H_P(\omega)$ given by (4), with 4-th order numerator and denominator, can be written:

$$H_{Pi}(\omega) = \left(\omega^4 + b_{1i} \cdot \omega^2 + b_{0i}\right) \Big/ \left(\omega^4 + a_{1i} \cdot \omega^2 + a_{0i}\right) \quad (5)$$

As specified earlier, ω is the frequency normalized to the cut-off frequency ω_0; finally, ω is substituted by ω/ω_0 in (5). It is more convenient to substitute ω by $p \cdot \omega$, where $p = 1/\omega_0$. Thus the ratio factor $H_{Pi}(\omega)$ from (5) can be re-written in the following form including the parameter *p*, which makes it scalable along the frequency axis:

$$H_{Pi}(\omega) = \left(p^4\omega^4 + b_{1i} \cdot p^2\omega^2 + b_{0i}\right) \Big/ \left(p^4\omega^4 + a_{1i} \cdot p^2\omega^2 + a_{0i}\right) \quad (6)$$

For a given value $p \neq 1$, the characteristic $H_P(\omega)$ displayed in Fig. 1 (b) either stretches (for $p < 1$) or shrinks (for $p > 1$) along the frequency axis. In Fig. 1 (c), (d) two low-pass characteristics derived from $H_P(\omega)$ are plotted, for the indicated values of *p* and ω_0. Thus the 1D prototype is parametric depending on *p*. From the two proposed prototypes, $H_1(\omega)$ given by (2) is maximally-flat and simpler, but its bandwidth is fixed and can only be used in a few particular cases, as shown further in Section 3. The prototype $H_P(\omega)$ given by (4) has a higher order, but it has the advantage of being scalable. Thus it is more general and will be used in some design examples in Section 4.

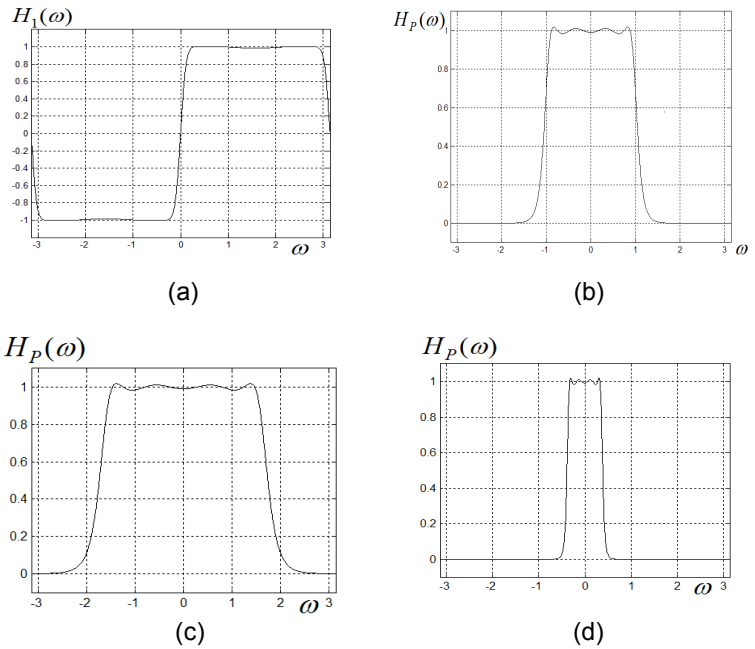

Fig. 1. (a) Odd-parity function $H_1(\omega)$; (b) LP prototype filter for $p = 1$ $(\omega_0 = 1)$; (c), (d) scaled LP filter for $p = 0.6$ $(\omega_0 = 0.53\pi)$ and $p = 2.7$ $(\omega_0 = 0.118\pi)$

3. DIAMOND AND FAN-SHAPED 2D FILTER DESIGN

Some simple 2D IIR filters with diamond, fan and wedge-shaped characteristics will be next designed using frequency mappings applied to the zero-phase LP prototype filter given by (2). By making the substitution $\omega \to (\omega_1 + \omega_2)/2$ in (2), a diagonal unilateral filter results, as shown in Fig. 2 (b):

$$H_{U1}(\omega_1,\omega_2) = H_P\left((\omega_1+\omega_2)/2\right) = \frac{1.265\cdot\sin\left((\omega_1+\omega_2)/2\right)\cdot\left(1-0.687922\cos(\omega_1+\omega_2)\right)}{\left(1-1.062289\cos(\omega_1+\omega_2)+0.105738\cos 2(\omega_1+\omega_2)\right)} \\ = 1.265\cdot\sin\left((\omega_1+\omega_2)/2\right)\cdot H_{PE}(\omega_1+\omega_2) \tag{7}$$

where $H_{PE}(\omega_1+\omega_2)$ is the even part of the unilateral response $H_{U1}(\omega_1,\omega_2)$. Likewise, making the substitution $\omega \to (\omega_1-\omega_2)/2$, another diagonal unilateral filter results:

$$H_{U2}(\omega_1,\omega_2) = H_P\left((\omega_1-\omega_2)/2\right) = 1.265\cdot\sin\left((\omega_1-\omega_2)/2\right)\cdot H_{PE}(\omega_1-\omega_2) \tag{8}$$

The frequency response $H_{U2}(\omega_1,\omega_2)$ is $H_{U1}(\omega_1,\omega_2)$ rotated with $\pi/2$ in the frequency plane. Obviously the factors $\sin\left((\omega_1+\omega_2)/2\right)$ and $\sin\left((\omega_1-\omega_2)/2\right)$ from (7) and (8) can only be implemented by means of interpolation. However, the product of functions $H_{U1}(\omega_1,\omega_2)$, $H_{U2}(\omega_1,\omega_2)$ represents the frequency response of a fan filter as follows:

$$H_{F1}(\omega_1,\omega_2) = H_{U1}(\omega_1,\omega_2)\cdot H_{U2}(\omega_1,\omega_2) \tag{9}$$

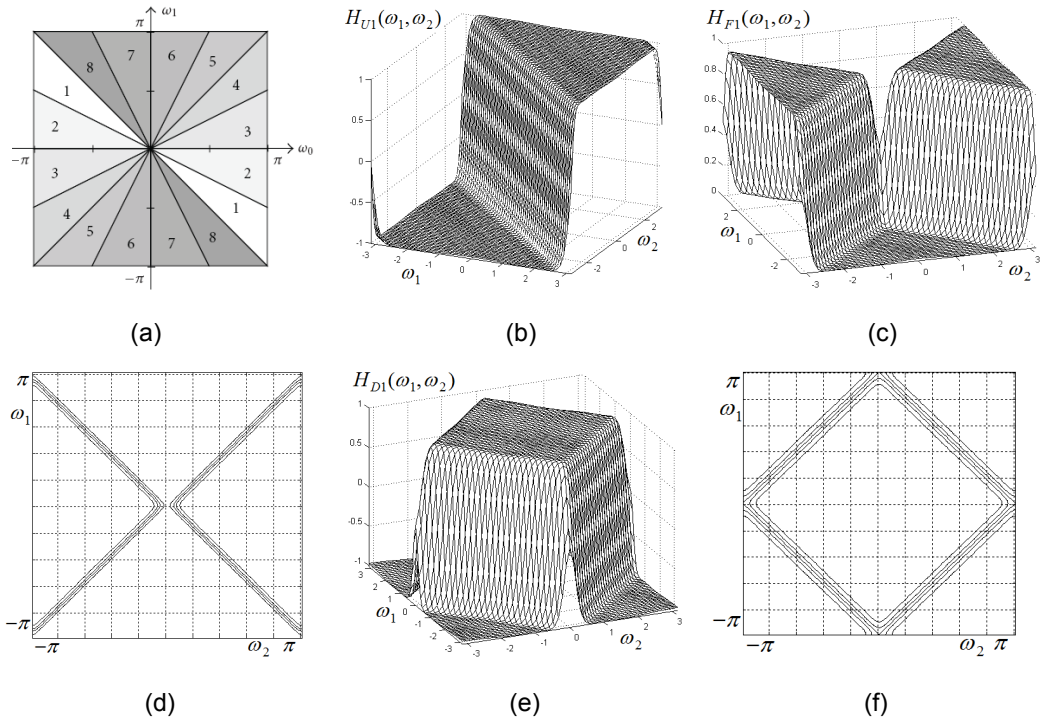

Fig. 2. (a) 8-band frequency plane partition; frequency response and contour for: (b) diagonal unilateral filter; (c), (d) fan filter; (e), (f) diamond filter

and using the identity $\sin\left((\omega_1-\omega_2)/2\right)\cdot\sin\left((\omega_1-\omega_2)/2\right)=(\cos\omega_2-\cos\omega_1)/2$, the frequency response of the fan filter shown in Fig. 2 (c) is given by:

$$H_{F1}(\omega_1,\omega_2)=0.8\cdot(\cos\omega_2-\cos\omega_1)\cdot H_{PE}(\omega_1-\omega_2)\cdot H_{PE}(\omega_1+\omega_2) \tag{10}$$

From this fan filter it is straightforward to derive a diamond filter. As shows the frequency response in Fig. 2 (e), it simply results by shifting the fan filter in Fig. 2 (c) along the axis ω_1 with the values $\pm\pi$. Its frequency response $H_{D1}(\omega_1,\omega_2)$ is:

$$H_{D1}(\omega_1,\omega_2)=H_{F1}(\omega_1+\pi,\omega_2)=0.8\cdot(\cos\omega_2+\cos\omega_1)\cdot H_{PE}(\omega_1+\pi-\omega_2)\cdot H_{PE}(\omega_1+\pi+\omega_2) \tag{11}$$

Substituting ω in (2) by ω_1 and ω_2 , we derive the frequency responses $H_{U12}(\omega_1,\omega_2)=H_1(\omega_1)$, $H_{U22}(\omega_1,\omega_2)=H_1(\omega_2)$ of the half-plane unilateral filters shown in Fig. 3 (a), (b).

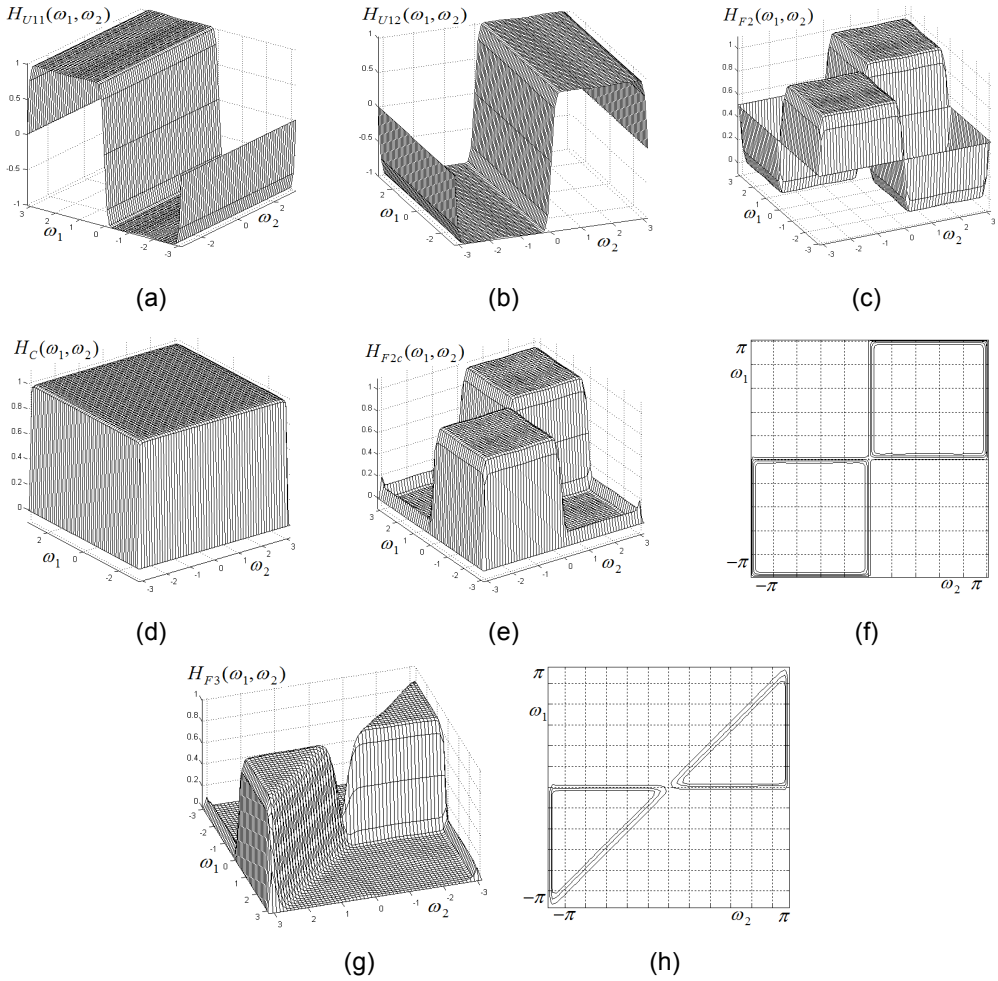

Fig. 3. Frequency responses and contour plots for: (a), (b) unilateral filters; (c) uncorrected odd-symmetry fan filter; (d) square LP correction filter; (e), (f) corrected odd-symmetry fan filter; (g), (h) half-quadrant wedge-filter

Using these frequency responses, the fan filter $H_{F2}(\omega_1,\omega_2)$ displayed in Fig. 3 (c) results, with the frequency response given by the expression:

$$H_{F2}(\omega_1,\omega_2)=0.5\cdot\left(1+H_{U12}(\omega_2)\cdot H_{U22}(\omega_1)\right) \quad (12)$$

As can be noticed, this filter has some marginal residual distortions due to periodicity in the frequency plane. These are subsequently removed by applying an additional correction low-pass filter $H_C(\omega_1,\omega_2)$ with large pass-bandwidth, like in Fig. 3 (d).

This square-shaped low-pass correction filter is based on a simple prototype having the rational expression $H_C(\omega)=k\cdot(1+\cos\omega)\big/\left(k\cdot(1+\cos\omega)+1\right)$; for larger values of *k*, the filter is steeper and with larger bandwidth. The 2D low-pass filter results as: $H_C(\omega_1,\omega_2)=H_C(\omega_1)\cdot H_C(\omega_2)$ and is separable. The filter in Fig. 3 (d) results for the parameter value $k=100$.

The corrected fan filter shown in Fig.3 (e), (f) has the frequency response of the form $H_{F2C}(\omega_1,\omega_2)=H_{F2}(\omega_1,\omega_2)\cdot H_C(\omega_1,\omega_2)$ and the marginal distortions are visibly reduced. The frequency response $H_{F3}(\omega_1,\omega_2)$ of a half-quadrant wedge filter, shown in Fig. 3 (g), (h), results as the product $H_{F3}(\omega_1,\omega_2)=H_{F1}(\omega_1,\omega_2)\cdot H_{F2C}(\omega_1,\omega_2)$, i.e. multiplying the filter frequency responses displayed in Fig. 2 (c) and Fig. 3 (e).

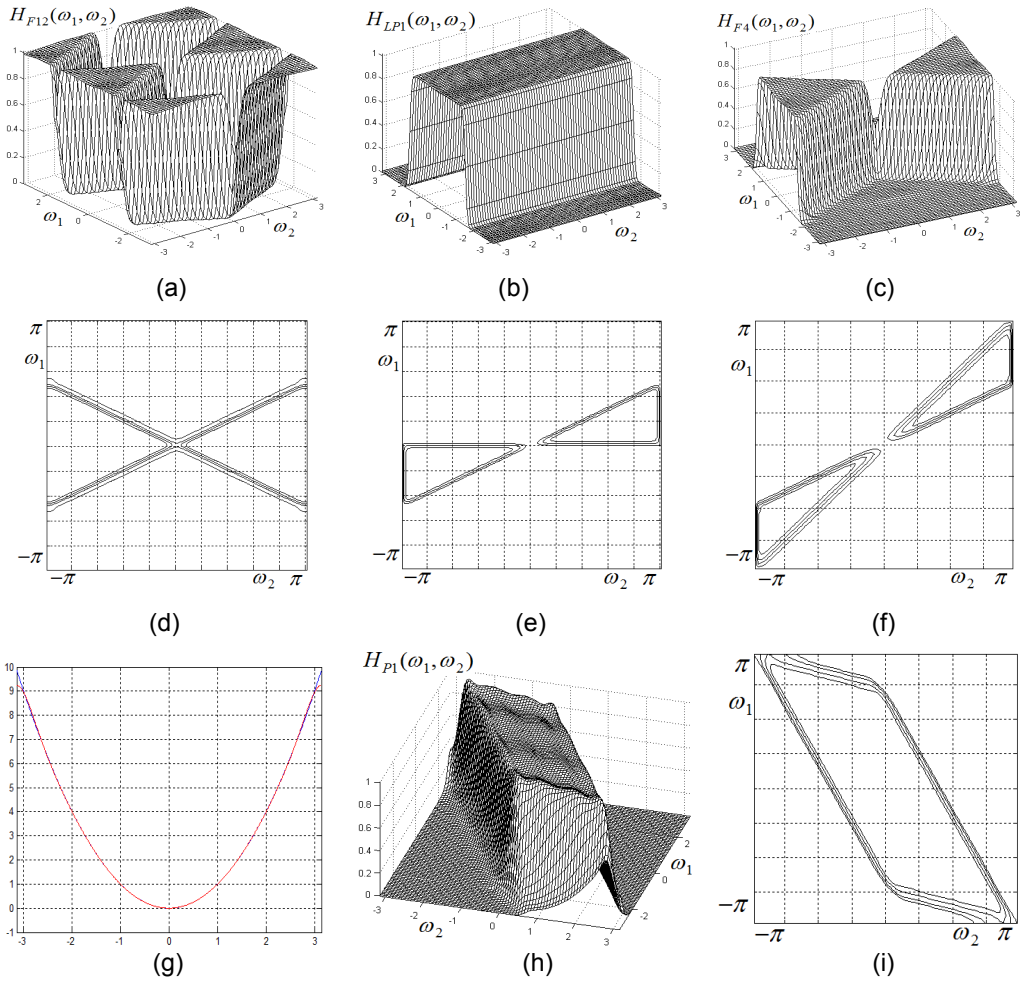

Fig. 4. (a) contracted fan filter; (b) LP filter; (c), (d) narrower fan filter; quarter-quadrant filters: (e) $H_{F5}(\omega_1,\omega_2)$; (f) $H_{F6}(\omega_1,\omega_2)$; (g) The function ω^2 (in blue) and its trigonometric approximation (in red); (h), (i) parallelogram-shaped 2D filter

A low-pass filter can be derived from the unilateral function $H_{U12}(\omega_1,\omega_2)$ through the frequency shift $\omega_1 \to \omega_1 + \pi$, resulting in $H_{LP1}(\omega_1,\omega_2) = 0.5\cdot\left(1+H_1(\omega_1+\pi)\right)$, which is displayed in Fig. 4 (b).

From $H_{F1}(\omega_1,\omega_2)$ shown in Fig. 2 (c), a fan filter contracted along ω_1 axis results, having the frequency response given in Fig. 4 (a), with the expression:

$$H_{F12}(\omega_1,\omega_2) = 0.5\cdot\left(1+H_1(\omega_1+2\omega_2)\cdot H_1(\omega_1-2\omega_2)\right) \quad (13)$$

Using the LP filter in Fig. 4 (b) to remove undesired spectra, the narrower fan filter shown in Fig. 4 (c), (d) results, given by:

$$H_{F4}(\omega_1,\omega_2) = H_{F12}(\omega_1,\omega_2)\cdot H_{LP1}(\omega_1,\omega_2) \quad (14)$$

Finally two quarter-quadrant wedge filters are derived, whose contour plots are displayed in Fig. 4 (e), (f). Their frequency responses are given by the expressions $H_{F5}(\omega_1,\omega_2) = H_{F4}(\omega_1,\omega_2)\cdot H_{F2C}(\omega_1,\omega_2)$ and $H_{F6}(\omega_1,\omega_2) = H_{F3}(\omega_1,\omega_2) - H_{F5}(\omega_1,\omega_2)$, respectively. Using successively this method, more selective filters of this type may be obtained.

4. PARALLELOGRAM AND WEDGE-SHAPED FILTER DESIGN

In this section a design method for parallelogram and wedge-shaped 2D IIR filters is proposed, using frequency transformations applied to the scalable low-pass prototype (4). From a 1D prototype filter $H_P(s) = H_P(j\omega)$ (varying on one axis only), a 2D oriented filter results by rotating the axes of the plane (ω_1,ω_2) by an angle φ . The rotation is defined by the linear transformation, where ω_1,ω_2 are the original frequency variables and $\overline{\omega}_1,\overline{\omega}_2$ the new ones [1]:

$$\begin{bmatrix}\omega_1\\ \omega_2\end{bmatrix} = \begin{bmatrix}\cos\varphi & \sin\varphi\\ -\sin\varphi & \cos\varphi\end{bmatrix}\cdot\begin{bmatrix}\overline{\omega}_1\\ \overline{\omega}_2\end{bmatrix} \quad (15)$$

The spatial orientation is specified by an angle φ about ω_1 axis, and defined by the 1D to 2D frequency mapping [1]:

$$\omega \to \omega_1\cos\varphi + \omega_2\sin\varphi \quad (16)$$

Squaring both members of mapping (16), we obtain:

$$\omega^2 \to p_1\cdot\omega_1^2 + p_2\cdot\omega_2^2 + p_{12}\cdot(\omega_1+\omega_2)^2 \quad (17)$$

where the parameters occurring in (17) have the following expressions: $p_1 = 0.5\cdot(1+\cos 2\varphi - \sin 2\varphi)$, $p_2 = 0.5\cdot(1-\cos 2\varphi - \sin 2\varphi)$, $p_{12} = 0.5\cdot\sin 2\varphi$, depending on the value of angle φ . Substituting the mapping given by (17) into the adjustable LP prototype (4), a rational expression in powers of ω_1^2 , ω_2^2 and $(\omega_1+\omega_2)^2$ is found. The next step is to find convenient trigonometric expressions for these terms. Using the variable change $\omega = \arccos(x/\pi) \leftrightarrow x = \pi\cos(\omega)$ and the Chebyshev-Padé method, we can easily derive:

$$\omega^2 \cong 1.3451\cdot\frac{(1-0.31518\cdot\cos\omega - 0.68117\cdot\cos 2\omega)}{(1+0.99346\cdot\cos\omega + 0.08573\cdot\cos 2\omega)} \quad (18)$$

which is a very accurate approximation, plotted in Fig. 4 (g). The parallelogram-shaped filter in Fig. 4 (h), (i) has a frequency response $H_{P1}(\omega_1,\omega_2)$ resulted as a product between frequency responses of two oriented filters with parameters $p = 0.96$, $\varphi = \pi/6$ and $p = 0.46$, $\varphi = \pi/12$, respectively. In this example, two opposite corners of the parallelogram are located in two opposite corners of the frequency plane.

From the parallelogram-shaped filter $H_{P1}(\omega_1,\omega_2)$, a wedge filter $H_{W1}(\omega_1,\omega_2)$ is derived if its frequency response is shifted by the value π along both frequency axes ω_1 , ω_2 :

$$H_{W1}(\omega_1,\omega_2) = H_{P1}(\omega_1+\pi,\omega_2+\pi) \quad (19)$$

5. DISCUSSION

The stability of the designed filters will be studied in further work. Generally, the problem of ensuring stability for 2D filters is much more complicated than for 1D filters. However, if the 1D prototype used in design is stable and the applied frequency mappings preserve stability, the obtained 2D filters should also be stable.

However, various stability criteria have been established [6] and stabilization methods can be applied for unstable filters [7].

As regards comparison with previous work on this topic, the novelty of the proposed method consists in using efficient, zero-phase scalable prototype filters, to which specific frequency mappings are applied, which lead to 2D filters with desired shapes. Based directly on the prototypes proposed by the author, elementary diamond and fan-shaped filters are obtained, then these are combined successively, using symmetry properties as well, in order to derive more selective filters of this type, for instance fan filters with a smaller aperture angle, i.e. with higher angular selectivity. Thus, these filters can be regarded as components of directional filter banks, as they realize a partitioning of the frequency plane into a given number of fan-shaped regions. Such filter banks are used in pattern recognition applications, in particular detecting and separating objects with a given orientation in the image to be processed. The author basically proposed here a novel, efficient approach to solve the problem of frequency plane partitioning. The analytical design method presented here is relatively simple and efficient, leading to accurate 2D filters with high selectivity and relatively low order, which is a major advantage in implementation.

6. CONCLUSION

The proposed analytical design method is simple and efficient, yielding 2D IIR zero-phase filters which can select in the frequency plane regions of various shapes, for instance parallelogram, diamond, fan or wedge-type. As shown, more selective 2D filters (which select narrower regions of the frequency plane) result by combining more elementary filters, in other words by multiplying their frequency responses. The derived 2D filters, as the presented design examples show, have maximally-flat characteristics, steep transition, an accurate shape with low distortions and high selectivity, which allows for a precise partitioning of the frequency plane into regions with desired shape. These may be used in 2D filter banks which are applied in image classification tasks.

COMPETING INTERESTS

Author has declared that no competing interests exist.

REFERENCES

1. Lu WS, Antoniou A. Two-dimensional digital filters. CRC Press; 1992.
2. Najim M. (Editor). Digital filters design for signal and image processing. Wiley; 2006.
3. Chakrabarti S, Mitra SK. Design of two-dimensional digital filters via spectral transformations. Proceedings of the IEEE. 1977;65(6):905-914.
4. Hirano K, Aggarwal JK. Design of two-dimensional recursive digital filters. IEEE Transactions on Circuits and Systems. 1978;CAS-25:1066-1076.
5. Zhu WP, Ahmad MO, Swamy MNS. A least-square design approach for 2D FIR filters with arbitrary frequency response. IEEE Transactions on Circuits and Systems II. 1999;46(8):1027-1034.
   DOI: 10.1109/82.782044
6. O'connor BT, Huang TS. Stability of general two-dimensional recursive digital filters. IEEE Transactions on Acoustics, Speech and Signal Processing. 1978;26 (6):550–560.
   DOI: 10.1109/TASSP.1978.1163162
7. Damera-Venkata N, Venkataraman M, Hrishikesh MS, Reddy PS. Stabilization of 2-D recursive digital filters by the DHT method. IEEE Transactions on Circuits and Systems II. 1999;46(1):85-88.
   DOI: 10.1109/82.749104
8. Tosic DV, Mojsilovic A, Popovic M. Symbolic approach to 2D biorthogonal diamond shaped filter design. 21st Int. Conference on Microelectronics, Nis, Yugoslavia. 1997;2:709-712.
   DOI: 10.1109/ICMEL.1997.632943
9. Low SH, Lim YC. A new approach to design sharp diamond-shaped filters. Signal Processing. 1998;67(1):35-48.
   DOI: 10.1016/S0165-1684(98)00020-6
10. Lim YC, Low SH. The synthesis of sharp diamond-shaped filters using the frequency response masking approach. IEEE Int. Conf. on Acoustics, Speech & Signal Processing ICASSP'97, Munich. 1997;3:2181-2184.
    DOI: 10.1109/ICASSP.1997.599481
11. Park SI, Smith MJT, Mersereau RM. A new directional filter bank for image analysis and classification. IEEE Int. Conf. on Acoustics, Speech and Signal Processing ICASSP'99, Phoenix, Arizona.

1999;3:1417-1420.
DOI: 10.1109/ICASSP.1999.756247
12. Bamberger RH, Smith MJT. A filter bank for the directional decomposition of images: Theory and design. IEEE Transactions on Signal Processing. 1992; 40(4):882-893
DOI: 10.1109/78.127960
13. Liang L, Shi G, Xie X. Nonuniform directional filter banks with arbitrary frequency partitioning. IEEE Trans Image Process. 2011;20(1):283-8.
DOI: 10.1109/TIP.2010.2052267
14. Shi G, Liang L, Xie X. Design of directional filter banks with arbitrary number of subbands. IEEE Transactions on Signal Processing. 2009;57(12):4936-4941.
DOI: 10.1109/TSP.2009.2027737
15. Ansari R. Efficient IIR. FIR fan filters. IEEE Transactions on Circuits and Systems. 1987;34(8):941-945.
DOI: 10.1109/TCS.1987.1086224
16. Weiping Z, Nakamura S. An efficient approach for the synthesis of 2-D recursive fan filters using 1-D prototypes. IEEE Transactions on Signal Processing. 1996;44(4):979-983.
DOI: 10.1109/78.492549
17. Matei R. Design of adjustable square-shaped 2D IIR filters. ISRN Signal Processing, Hindawi; 2013.
Article ID 796830
18. Matei R. Design method for wedge-shaped filters. Int. Conference on Signal Processing and Multimedia Applications SIGMAP, Milano, Italy. 2009;19-23.

Peer-review history:
The peer review history for this paper can be accessed here:
http://sciencedomain.org/review-history/16784